Colloids and Surfaces B: Biointerfaces 158 (2017) 25–32

Contents lists available at ScienceDirect

Colloids and Surfaces B: Biointerfaces

journal homepage: www.elsevier.com/locate/colsurfb

Protocols

Gold nanoparticles as an efficient drug delivery system for GLP-1 peptides

Magdalena Pérez-Ortiz[a,b,1], Claudio Zapata-Urzúa[a,b,1], Gerardo A. Acosta[b,c,d], Alejandro Álvarez-Lueje[a,*], Fernando Albericio[b,c,d,e,**], Marcelo J. Kogan[a,f,*]

[a] Faculty of Chemical and Pharmaceutical Sciences, University of Chile, Sergio Livingstone 1007, Independencia, Santiago, Chile
[b] Institute for Research in Biomedicine, University of Barcelona Baldiri Reixac 10, Barcelona 08028, Spain
[c] CIBER-BBN, Networking Centre on Bioengineering, Biomaterials and Nanomedicine, Barcelona Science Park, Barcelona 08028, Spain
[d] Department of Organic Chemistry, University of Barcelona, Martí i Franquès 1, Barcelona 08028, Spain
[e] School of Chemistry and Physics, University of KwaZulu-Natal, Durban 4001, South Africa
[f] Advanced Center for Chronic Diseases, Sergio Livingstone 1007, Independencia, Santiago, Chile

ARTICLE INFO

Article history:
Received 24 November 2016
Received in revised form 31 May 2017
Accepted 17 June 2017
Available online 19 June 2017

Keywords:
GLP-1
Gold nanoparticles
Caco-2 cells
Solid-phase peptide synthesis
Incretin

ABSTRACT

In this work, the potential application of gold nanoparticles for GLP-1 analogues delivery was studied. For this purpose, the original sequence of the incretin GLP-1 was slightly modified in the C-terminal region by adding a cysteine residue to facilitate conjugation to the gold surface. The interaction between peptides and gold nanoparticles and also the colloid stability of the conjugates were studied by UV–vis spectrophotometry, TEM, IR and XPS spectroscopy. Moreover, the permeability of these conjugates was assayed using a Caco-2/goblet monolayer model. On the basis of the stability and permeability results, one of the conjugates was chosen to be administered intraperitoneally to normoglycemic rats. The intraperitoneal delivery of the GLP-1 analogue using gold nanoparticles led to decrease levels of blood glucose in the same way as native GLP-1, thereby demonstrating that the formulation of the analogue is stable in physiological conditions and maintains the activity of this incretin.

1. Introduction

Glucagon like peptide-1 (GLP-1) is an incretin hormone secreted by intestinal L cells in response to nutrient intake. It has two biological active forms: GLP-1 (7–36) amide {80% of circulating GLP-1} and GLP-1 (7–37) [1]. GLP-1 and its analogues induce pleiotropic physiological effects manifested via the stimulation of glucose-dependent insulin secretion and insulin biosynthesis, the inhibition of glucagon secretion, reduced appetite, and delayed gastric emptying. In addition, these peptides support prolonged normoglycemia, preserve β-cell function, increase insulin sensitivity, improve cardiac function, decrease blood pressure, improve lipid profiles, reverse fatty liver, and reduce oxidative stress [2]. For these reasons, currently GLP-1 is not only important for its therapeutic potential for the treatment of type 2 diabetes mellitus but it is also emerging as a new strategy for the treatment of other non-communicable chronic diseases related to diabetes and the metabolic syndrome. However, like other peptides, GLP-1 and its analogues present a major drawback with respect to stability in order to be considered as drugs. In this regard, most of the effects of GLP-1 *in vivo* last for a brief period of time ($t_{1/2}$ < 2 min) because it is rapidly inactivated by dipeptidyl peptidase-4 (DPP-4).

Several strategies have been developed to increase the half-life of GLP-1 and achieve clinical use, including exendin-based therapies, DPP-4-resistant analogues, and analogues of human GLP-1 [3]. Currently, there are three commercially available analogues, namely exenatide immediate-release, exenatide extended-release (long-acting), and liraglutide. However, all of these drugs are marketed in injectable dosage form only [4].

A non-invasive route of administration for GLP-1 or its analogues would augment patient compliance and acceptability, while oral delivery, in addition, would preserve the portal/peripheral ratios naturally experienced upon the secretion of this incretin, thereby more closely mimicking its physiological state.

However, oral peptide delivery is a challenge for the pharmaceutical industry, since peptides have low oral bioavailability due to

* Corresponding authors at: Faculty of Chemical and Pharmaceutical Sciences, University of Chile, Sergio Livingstone 1007, Independencia, Santiago, Chile.
** Corresponding author at: University of Barcelona, Martí i Franquès 1, Barcelona 08028, Spain.
E-mail addresses: aalvarrez@ciq.uchile.cl (A. Álvarez-Lueje), albericio@ub.edu (F. Albericio), mkogan@ciq.uchile.cl (M.J. Kogan).
[1] These authors contributed equally.

http://dx.doi.org/10.1016/j.colsurfb.2017.06.015
0927-7765/

their poor permeability and low stability under physiological conditions. Thus, permeation enhancers, protease inhibitors, enteric coatings and novel carrier systems have all been employed, with varying degrees of success, for the development of non-invasive biomolecule formulations [5–7]. Among these, nanoscale devices have shown new and improved pharmacokinetic and pharmacodynamics properties (enhanced bioavailability, high drug loading and systemic stability) when used as drug delivery systems [8]. In this regard, gold nanoparticles (AuNPs) could be considered ideal agents for this purpose because of their chemical inertness and minimal toxicity [9–12]. Additionally, in contrast to organic colloids, the surface of colloidal gold does not require modification for the chemisorption of ligands. Thus, AuNPs can be functionalized easily with a variety of biomolecules such as peptides, proteins, enzymes and DNA, and also small molecule-based drugs. These AuNP-based conjugates retain the activity of the cargo, improve its stability, and reduce dose and also possible side effects [13]. AuNPs are more effective as drug delivery systems than the traditional naked drug as they can reduce drug delivery time significantly, improve cell penetration, and enhance the pharmacodynamic activity [14–18]. As example, Joshi et al. observed an extraordinary reduction of blood glucose levels of diabetic rats when insulin was delivered by AuNPs via both the transmucosal and oral route [19,20].

Nevertheless, despite the large number of studies that have demonstrated that AuNPs are non-toxic to living cells, biocompatible, and easily conjugated to a spectrum of biological ligands, reports on their application for drug delivery purposes have been limited to cancer therapies [8,16–18,21].

In this work, three new analogues of incretin GLP-1 were synthesized in order to facilitate attachment to AuNPs. Peptides were characterized in terms of their secondary structure, ability to stimulate the release of insulin, and toxicity *in vitro*, while their AuNP conjugates were also fully characterized in terms of size, charge, peptide loading, and stability. The permeability of peptide-AuNP conjugates across Caco-2 cells and toxicity were also examined *in vitro*. The interaction of these peptides with the gold surface was studied by XPS and IR spectroscopy. Also, the way in which this interaction affected the stability and permeability of the conjugates was studied. Finally, to test the efficacy of this new potential delivery system, the effect of one of the three conjugates on blood glucose levels was tested in normoglycemic mice and compared with the respective free GLP-1 analogue and the native GLP-1.

2. Experimental section

2.1. Synthesis of gold nanoparticles

AuNPs were synthesized by reducing $HAuCl_4$ with sodium citrate, 1:4 molar ratio, as described in a previous study [22].

2.2. Characterization of gold nanoparticles and conjugates

Bare AuNPs and AuNPs conjugated to GLP-1 analogues were studied by spectrophotometry, transmission electron microscopy (TEM), infrared spectroscopy (IR), X-ray photoelectron spectroscopy (XPS), dynamic light scattering (DLS) [23] and zeta potential [24]. For details of each technique, see supporting information.

2.3. Estimation of the number of peptide molecules per AuNP

The peptide load of the AuNPs was calculated by dividing the amount of peptide grafted (determined by amino acid analysis) by the amount of AuNPs in solution, which was estimated following Liu et al. [25]. For this purpose, the number of gold atoms per nanoparticle, according to the size determined by TEM, and the concentration of gold in solution, obtained by ICP-OES, were considered. To determine peptide concentration, an amino acid analysis was performed on the pellet obtained after centrifugation of 10 mL of bare or conjugated AuNPs at $16100 \times g16100g$ for 30 and 60 min, respectively.

2.4. Conjugate stability

The colloidal stability of the non-functionalized and functionalized AuNPs was evaluated spectrophotometrically and by DLS in simulated gastric fluid (buffer solution pH 1.2), simulated intestinal fluid (buffer solution pH 6.8), HBSS, and saline solution (0.9% NaCl) for 96 h at room temperature. Simulated gastric and intestinal fluids were preparing following USP specifications [26].

2.5. In vivo *studies*

The capacity of free GLP-1(7–37)Lys(PEGCys)-NH_2 and GLP-1(7–37)Lys(PEGCys)-NH_2 conjugated to AuNPs to lower blood glucose was tested after intraperitoneal administration to normoglycemic rats. Male Sprague Dawley rats weighing 180–200 g were provided by the animal house of the Faculty of Chemical and Pharmaceutical Sciences of the University of Chile, Chile. The animals were housed at 25 °C under a 12/12 h light/dark cycle and fed a standard pellet diet with access to water *ad libitum*. Animal handling was performed following Good Laboratory Practices (GLPs). See supporting information for experimental details.

3. Results and discussion

3.1. Rational design of GLP-1 analogues for conjugation to AuNPs

GLP-1 activity is related to its N-terminal region and C-terminal amidation, which determine its interaction with GLP-1 receptor [27,28]. Additionally, amidation of GLP-1 protects it from degradation by carboxypeptidases present in the bloodstream, thus improving its stability [29].

Here we synthesized three analogues of GLP-1(7–37) with a slight modification at their C-terminal region in order to maintain stability against carboxypeptidases and facilitate conjugation to AuNPs (Table 1).

In the three peptides, a residue of amidated Lys was incorporated at the C-terminal to serve as a spacer between the peptide and the AuNP surface. In the second and third analogue, a residue of Cys was incorporated through the amino side chain of the Lys, directly or through a polyethylene glycol spacer (PEG). The Cys served to mediate the interaction with the AuNP surface through its thiol group. In contrast, in the first analogue the ε-amino function of the Lys was acetylated. This peptide was used as a reference to corroborate any other type of interaction with AuNPs and to study the effect of these interactions on the stability of the conjugates.

3.2. Peptide characterization and in vitro *biological activity*

After purification, the three products obtained had a chromatographic purity over 95% (Fig. SI-1). MALDI-TOF-MS was used to identify the corresponding quasi-molecular ions (Table SI-1). Using HPLC–MS, the mass-to-charge ratio (m/z) to the ionic species was found to be nearly identical to the theoretical m/z in each case (Table SI-2). The spectra obtained in the exact mass analysis confirm the chromatographic purity of the peptides and their molecular masses (Fig. SI-2).

To corroborate that the modifications made in the original sequence of GLP-1 do not alter its secondary structure, which is important for the interaction with GLP-1 receptor [30], circular dichroism (CD) analysis was performed for the three analogues in

Table 1
Sequences of the GLP-1(7–37) and GLP-1 analogues synthesized.

Peptides	Sequences
GLP-1(7–37)	His-Ala-Glu-Gly-Thr-Phe-Thr-Ser-Asp-Val-Ser-Ser-Tyr-Leu-Glu-Gly-Gln-Ala-Ala-Lys-Glu-Phe-Ile-Ala-Trp-Leu-Val-Lys-Gly-Arg-Gly-COOH
GLP-1(7–37)-Lys(Ac)-NH_2	His-Ala-Glu-Gly-Thr-Phe-Thr-Ser-Asp-Val-Ser-Ser-Tyr-Leu-Glu-Gly-Gln-Ala-Ala-Lys-Glu-Phe-Ile-Ala-Trp-Leu-Val-Lys-Gly-Arg-Gly-**Lys(Ac)-NH_2**
GLP-1(7–37)-Lys(Cys)-NH_2	His-Ala-Glu-Gly-Thr-Phe-Thr-Ser-Asp-Val-Ser-Ser-Tyr-Leu-Glu-Gly-Gln-Ala-Ala-Lys-Glu-Phe-Ile-Ala-Trp-Leu-Val-Lys-Gly-Arg-Gly-**Lys(Cys)-NH_2**
GLP-1(7–37)-Lys(PEGCys)-NH_2	His-Ala-Glu-Gly-Thr-Phe-Thr-Ser-Asp-Val-Ser-Ser-Tyr-Leu-Glu-Gly-Gln-Ala-Ala-Lys-Glu-Phe-Ile-Ala-Trp-Leu-Val-Lys-Gly-Arg-Gly-**Lys(Peg-Cys-)-NH_2**

water, PBS and various percentages of TFE. In all these conditions, the CD spectra of the peptides showed a characteristic α-helix pattern, as indicated by the presence of negative bands around 222 and 208 nm and a positive band at 190 nm (Fig. SI-3). Also, we observed that in PBS, the conformation of the three GLP-1 analogues comprised a combination of unordered, β sheet and α-helix structure (Table SI-3), as has been described for aqueous solutions of peptides of a similar size, which usually have relatively flexible and disordered structures, random coils and β sheets being the main components [31].

To determine the bioactivity of these new GLP-1 analogues, insulin secretion from β-TC6 cells was measured. As expected, in glucose-free medium, the cells did not show any significant release of insulin in response to GLP-1 or its analogues, even at a high concentration (100 nM) [32]. However, in the presence of 25 mM glucose, significant insulin secretion was observed after 30 and 120 min stimulation with all the peptides (100 nM). In this case, when the treatment was performed for 30 min, insulin secretion was detectable (average of 15 μg/L) but there was no difference between secretion in the presence and absence of the peptides or between them. In contrast, when the assay was carried out for 120 min, insulin levels reached 100 μg/L and clear differences were observed between those cells treated with peptides and those that were not (Fig. 1).

After 120 min, the three GLP-1 analogues stimulated the insulin release over four-fold that of the glucose control. There was no significant difference in potency between the analogues or between them and native GLP-1. Thus, our results demonstrated that the three analogues have insulinotropic effects on pancreatic cells and retain the biological activity of the native peptide at this level.

Additionally, none of the peptides had deleterious effects on β-TC6 cell viability at the concentration tested (100 nM), even after 16 h of treatment. This finding is in accordance with previous reports that indicate that GLP-1 has no toxic effects at the cellular level (Fig. SI-4) [2].

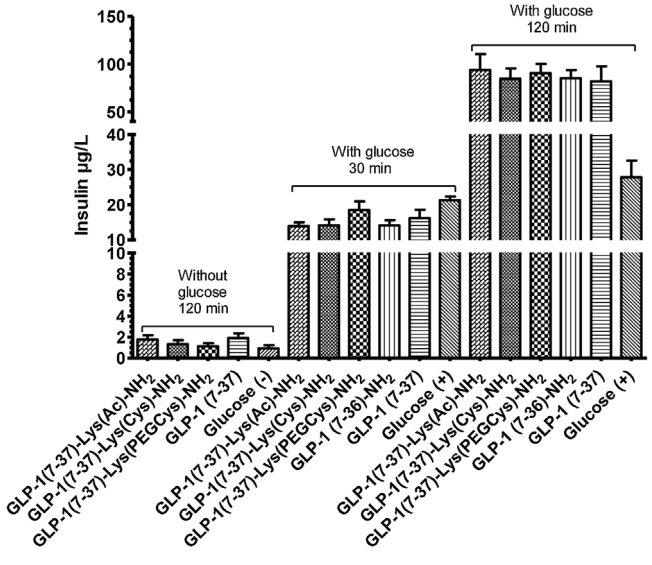

Fig. 1. Insulin levels obtained from the *in vitro* activity assays using β-TC6 cells. All the peptides were tested at 100 nM in the absence and presence of 25 mM glucose for 30 and 120 min. The graph corresponds to the results obtained in three independent experiments performed in triplicate, expressed as mean ± SEM. Statistical analysis: ANOVA, Tukey's Multiple Comparison Test.

3.3. Synthesis and characterization of AuNP-Peptide conjugates

The AuNPs synthesized had a surface plasmon resonance band of 519 ± 1 nm (n = 10) and a diameter of 12.7 ± 1.7 nm (n = 1000), as shown by TEM images (Fig. SI-5). Particles diameter was 20.4 ± 0.5 nm, as determined by DLS, and the Zeta-potential of AuNP dispersion at pH 9 was −46 ± 2 mV, thereby confirming the formation of a negatively charged surface in this citrate-stabilized gold dispersion. All these parameters were in accordance with previous reports [22,23].

Typically, the surface modification of AuNPs is reflected in a plasmon band shift to longer wavelengths due to the change that occurs in the refractive index and dielectric constant of the medium. The characteristic shift of the surface plasmon resonance band from 519 to about 527 nm was observed in the conjugates (Fig. 2). The change occurred within a few minutes, suggesting that the conjugation process is fast. In addition, no significant broadening of the spectra was seen after conjugation, thereby indicating that the interparticle distance was even greater than the particle radius and thus no significant aggregation occurred after adsorption of the peptides onto the AuNP surface [33]. The conjugates were stable for more than 6 months, as corroborated by UV–vis spectra (data not shown).

TEM analysis revealed a characteristic edge (thickness between 3 and 5 nm) on the surface of the nanomaterial with all GLP-1 analogues, confirming their conjugation to the AuNP surface (Fig. 3). Other changes that confirm the conjugation are shown in Table 2. No great differences in the Zeta-potential were

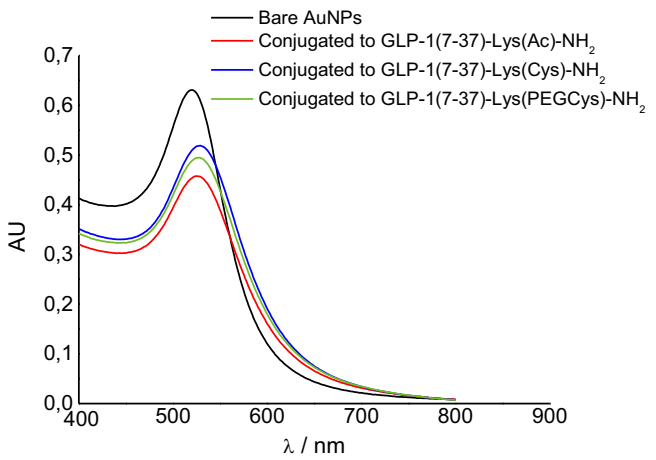

Fig. 2. Absorption spectra of bare AuNPs and AuNPs conjugated to GLP-1 analogues.

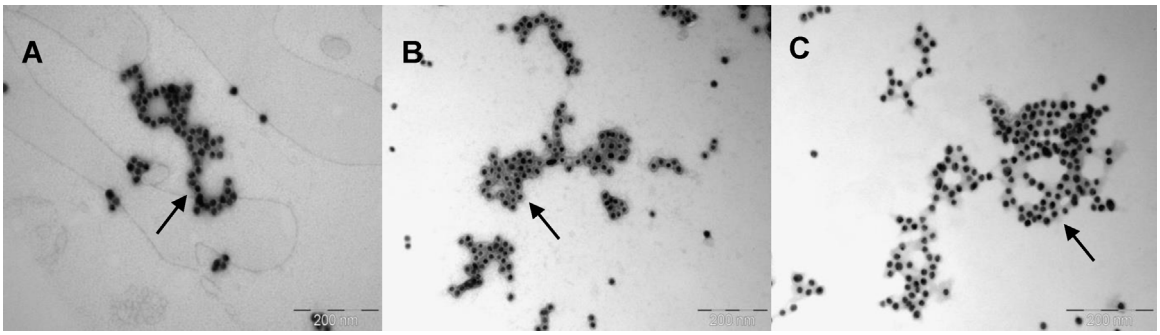

Fig. 3. TEM images of: (A) GLP-1(7–37)-Lys(Ac)-NH_2-AuNPs, (B) GLP-1(7–37)-Lys(Cys)-NH_2-AuNPs, (C) GLP-1(7–37)-Lys(PEGCys)-NH_2-AuNPs staining with uranyl acetate. The arrows indicate the characteristics edges produced by the presence of the peptides layers on the gold surfaces of the nanoparticles.

Table 2
Values of λ_{max} for the plasmon band, hydrodynamic diameter (D_H) and polydispersity index (PDI) obtained by DLS for bare AuNPs and AuNPs conjugated to GLP-1 analogues. Results are expressed as mean ± SD, n = 3.

AuNPs	UV-vis λ_{max} (nm)	DLS D_H (nm)[a]	DLS PDI	Zeta-Potential (mV)
Bare	519 ± 1	20.9 ± 1.0	0.214 ± 0.007	−46 ± 2
GLP-1(7–37)-Lys(Ac)-NH_2	526 ± 1	34.2 ± 2.0	0.369 ± 0.009	−38 ± 4
GLP-1(7–37)-Lys(Cys)-NH_2	528 ± 1	31.0 ± 1.0	0.308 ± 0.002	−41 ± 2
GLP-1(7–37)-Lys(PEGCys)-NH_2	528 ± 2	35.8 ± 1.3	0.329 ± 0.026	−41 ± 4

[a] D_H obtained from average intensity value.

appreciated between bare and conjugated AuNPs. This observation can be explained by the electrostatic nature of these molecules, which have three negative charges at pH 9.

The particle sizes obtained by TEM were smaller than those shown by DLS (Fig. 3 and Table 2). This finding is explained by the fact that the particle size obtained by DLS measurements included the solvent or stabilizer (GLP-1 analogues) added, thus determining the hydrodynamic diameter (D_H) of the particle. Moreover, the DLS method provides information on the size distribution of the different species present in the sample as aggregates. In this regard, the polydispersity index (PDI) by DLS was less than 0.4 but higher than 0.1 for all the conjugates, thereby indicating a moderately polydisperse distribution type [23]. However, no bimodal distribution was observed (Fig. 4).

Notably, it is important to mention that for AuNPs conjugated to GLP-1(7–37)-Lys(Ac)-NH_2 the highest PDI and the broadest particle size distribution (Fig. 4) was observed regarding to the AuNPs conjugated to Cys-containing peptides (GLP-1(7–37)-Lys(Cys)-NH_2 and GLP-1(7–37)-Lys(PEGCys)-NH_2). This observation could be attributed to a degree of interparticle aggregation. In this regard, in the case of GLP-1(7–37)-Lys(Cys)-NH_2 and GLP-1(7–37)-Lys(PEGCys)-NH_2, it is likely that Cys-modified peptides are chemisorbed mainly to the surface of AuNPs via the S-Au bond, which could facilitate the formation of an ordered monolayer in which the peptide molecules can be located orthogonally with respect to the gold surface, thus reducing interparticle interactions [22]. In contrast, when bare AuNPs (citrate-stabilized) were capped with GLP-1(7–37)-Lys(Ac)-NH_2, this peptide was not chemisorbed on the surface; however, other types of interaction would occur. In this regard, Lys and Arg residues can be protonated and interact electrostatically with the negatively charged AuNPs, whilst hydrogen bonding between peptide molecules and the citrate layer may also occur, as can hydrophobic interactions between the aromatic ring of phenylalanine and the gold surface [34]. Consequently, the peptide molecules are arranged in an unorderly fashion on the AuNP surface, thereby exposing the peptide residues to the solution and favoring interparticle aggregation.

We used a combination of IR spectroscopy and XPS to demonstrate that the peptides indeed form the ligand shell of the particles and to characterize the interactions that occur between peptide molecules and the AuNP surface (see Figs. SI-6, SI-7, SI-8, SI-9, SI-10, SI-11, SI-12 and Table SI-4, Supporting information). IR and XPS results revealed that AuNPs conjugated to GLP-1(7–37)-Lys(PEGCys)-NH_2 are better coated than those conjugated to GLP-1(7–37)-Lys(Cys)-NH_2 and considering the stability of this interaction would be more suitable for further *in vivo* studies.

3.4. Estimation of the number of peptide molecules per AuNP

According to the results (Table 3), thiolated peptides showed a higher degree of functionalization, which confirms that the interaction between the thiol group of Cys and that the metal surface is highly preferred. The low number of peptide molecules found in the case of GLP-1(7–37)Lys(Ac)-NH_2 could be due to the type of interaction between the peptide and gold surface, which would be weaker (electrostatic interaction and hydrogen bonding with the citrate layer) regarding S-Au binding. Therefore, some peptide molecules could have been lost during the centrifugation prior to amino acid analysis.

The difference between the two thiolated conjugates can be attributed to the presence of PEG, since this spacer would help to orient the molecules on the gold surface. Therefore, in the GLP-1(7–37)Lys(PEGCys)-NH_2 conjugate, peptide molecules would be arranged in an more orderly way on the surface of AuNPs than those of the GLP-1(7–37)Lys(Cys)-NH_2 conjugate, thus explaining the greater number of peptide molecules per AuNP found.

3.5. Stability of the conjugates

Given that the bonding nature between GLP-1 analogues and gold surface can affect the stability of the formulation, as well as determine the facility with which peptides are released from AuNPs, we studied the stability of the three colloidal systems following the changes in the plasmon band and D_H of AuNPs.

When bare AuNPs (citrate-capped) were resuspended in all the media assayed, the colloidal solution immediately changed colour from red to blue, thereby indicating the instability of this system. Absorbance at 519 nm became weaker and blue-shifted while a new broad band around 660 nm appeared due to dipole coupling between the plasmons of neighboring particles that were aggre-

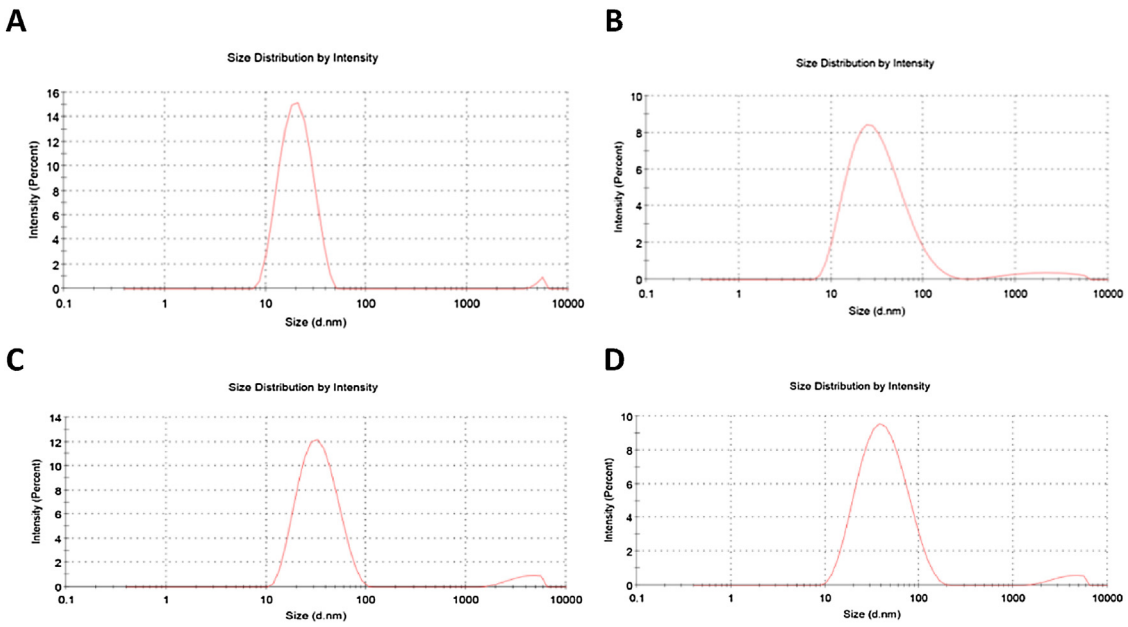

Fig. 4. Representative particle size distribution (PSD) determined by DLS for: (A) Bare AuNPs, (B) AuNPs conjugated to GLP-1(7–37)-Lys(Ac)-NH_2, (C) AuNPs conjugated to GLP-1(7–37)-Lys(Cys)-NH_2 and (D) AuNPs conjugated to GLP-1(7–37)-Lys(PEG-Cys)-NH_2.

Table 3
Concentration of AuNPs, peptides and number of peptide molecules per AuNP for the three conjugates. Results are expressed as mean± SD, n = 3.

Peptides	AuNP concentration (nM)	Peptide concentration (nM)	Peptide molecules per AuNP
GLP-1(1–37)-Lys(Ac)-NH_2	11.1 ± 0.4	4261 ± 255	383 ± 30
GLP-1(1–37)-Lys(Cys)-NH_2	11.6 ± 0.8	5926 ± 1323	515 ± 134
GLP-1(1–37)-Lys(PEGCys)-NH_2	11.0 ± 1.2	7396 ± 1619	673 ± 141

gated (Fig. SI-13A). In fact, particles settled completely in less than 4 h (Fig. SI-13B). DLS measurements confirmed this finding, since the D_H increased from approximately 20 nm to more than 300 nm in less than 30 min (Fig. SI-13C). This size increment led to particle aggregation, which was also reflected by the increase in polydispersity (Fig. SI-13D).

The low stability of bare AuNPs has been seen before, since colloidal stability is governed by the balance of Van der Waals attraction, double-layer repulsion and steric interaction forces, when these particles are suspended in media with a high concentration of electrolytes the thickness of the double layer decreases, making the attractive forces prevail over the repulsive. In addition, the absence of a high molecular weight molecule adsorbed or grafted onto their surface make no possible the steric stabilization. However, colloidal stability increases considerably when polymers or biomolecules are conjugated to these particles, as they provide immediate protection from electrolyte-induced aggregation [35].

When the GLP-1 analogues were conjugated to citrate-capped AuNPs, these colloids were much more stable, since the presence of the peptides on the surface formed a protective barrier that kept particles separated by mean of a steric effect additional to the electrostatic repulsion resulting from functional groups in the amino acid side chains. For this reason, the pH of the colloidal solution is crucial, as when the pH is close to the isoelectric point of peptides, which is about 7, the global charge will be near zero, thus reducing stability.

Although the three analogues of GLP-1 did not show large structural differences, the stability of their conjugates differed completely. The cysteine added to the thiolated peptides conferred a more stable interaction with AuNPs (by means of S-Au binding), thus keeping particles disperse and much more stable than the system stabilising with the peptide without cysteine (this can form only weak interactions, which can be broken easily when changes in the pH or medium composition occur).

Nevertheless, unlike bare AuNPs, AuNPs conjugated to GLP-1(7–37)Lys(Ac)-NH_2 were stable to centrifugation and resuspension, although bathochromic and hypochromic changes were observed by spectrophotometry after pellets were resuspended in the different media assayed (Fig. SI-14A, SI-14-B). Finally, after 8 h, these particles sedimented in all the conditions tested (Fig. SI-14). With the exception of particles in PBS, all the others were resuspended by means of slight shaking (data not shown).

Concomitant to the shift in the plasmon band, DLS showed an increment in the D_H from 35 nm (typical for AuNPs conjugated to GLP-1 analogues, see Table 2) to over 500 nm after 20 min, when AuNPs conjugated to GLP-1(7–37)Lys(Ac)-NH_2 were resuspended in any media (Fig. SI-14C). The increase in the size of the particles led to a decrease in the interparticle distance, thus causing particle aggregation and subsequent sedimentation of these AuNPs. However, the presence of the peptide on the AuNP surface prevented their complete aggregation. In this regard, they formed a kind of pink floccule, thus allowing their re-suspension after precipitation. This observation contrasts with bare AuNPs, which formed a blue "cake" that could not be resuspended.

Thiolated peptide colloids proved to be considerably more stable than the previous ones, as reflected in the stability of their plasmon band and D_H (Figs. SI-15A and SI-16A). When AuNPs were conjugated to GLP-1(7–37)-Lys(Cys)-NH_2 or GLP-1(7–37)-Lys(PEGCys)-NH_2, the plasmon band range between 525 and 527 nm, except when AuNPs conjugated to GLP-1(7–37)-Lys(PEGCys)-NH_2 were resuspended in simulated intestinal medium (SIM) at pH 6.8. In this medium a shift of the plasmon band was observed after 4 h, which corresponded to a slight increase in D_H (Fig. SI-16). A similar increment in D_H was observed when these

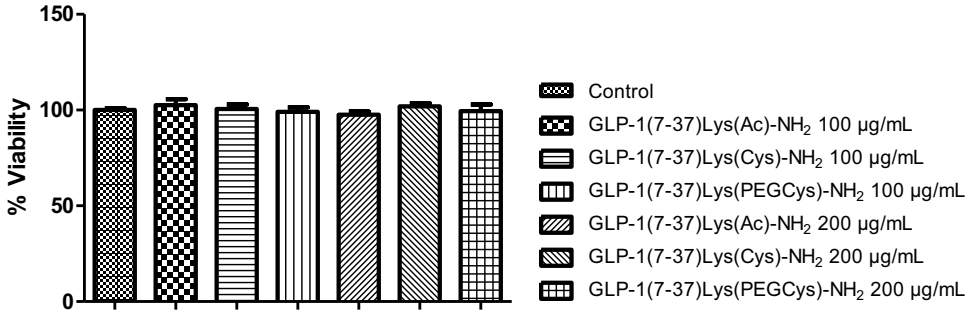

Fig. 5. Caco-2 cell viability assay after 4 h of treatment with conjugates of AuNP-GLP-1 analogues. Results are expressed as mean± SEM, n = 3.

particles were resuspended in simulated gastric medium (SGM) at pH 1.2; however, in this case no shift in the plasmon band was detected. In all the other conditions, the hydrodynamic diameter remained around 35 nm for both thiolated conjugates. In addition, it is important to mention that these particles were stable for more than 96 h.

The high stability of AuNPs conjugated to the thiolated peptides, even at pH near their isoelectric point, would be provided largely by the steric stabilization that the peptide molecules confer to the system, in spite of the presence of a minimum electrostatic effect. Additionally, these particles showed an uncommon stability in SGM, as under these pH conditions both peptides had a positive net charge (pI ∼ 7), as revealed by Zeta-potential measurements, where AuNPs conjugated to GLP-1(7–37)Lys(Cys)-NH_2 and GLP-1(7–37)-Lys(PEGCys)-NH_2 showed values of +26 ± 2 mV and +28 ± 2 mV, respectively.

3.6. *Permeability assay*

In the *in vitro* permeability assay (carried out for 2 h), as we expected, free peptides could not be detected in the basolateral compartments. However, neither did we detect AuNPs in the basolateral side in the case of the conjugates. In this case, a large amount of gold remained in the apical chamber and very low amounts were detected in the filters that held the cell monolayers (Table SI-5).

Remarkably, increasing the concentration of gold in the apical compartment did not increase its retention in the cell monolayer samples. In fact, gold retention remained the same for thiolated conjugates, while it tended to decrease for the conjugate of GLP1(7–37)Lys(Ac)-NH_2. These results could be explained by a saturable transport mechanism, which would be involved in the cell uptake of AuNP conjugates (Table SI-5).

After 2 h, practically no differences in gold retention inside cells were observed between conjugates of the two thiolated peptides in the range of concentrations assayed (∼0.002% of gold retention). However, a slight difference between the conjugates of these two thiolated peptides and those of AuNPs conjugated to GLP-1(7–37)Lys(Ac)-NH_2 was detected. Conjugates of GLP-1(7–37)Lys(Ac)-NH_2 showed a higher concentration of gold in cell monolayers, with 0.006, 0.004 and 0.003% of gold retention when concentrations of this metal of about 60, 100 and 200 μg/mL, respectively, were assayed, whilst conjugates of thiolated peptides did not exceed 0.003% at similar concentrations (Table SI-5).

In view of these results, we assayed the permeability of the conjugates after 4 h at a gold concentration of 100 and 200 μg/mL; however, again it was impossible to detect gold in the basal compartment, although an increase in gold retention by cell monolayers treated with GLP-1(7–37)Lys(Ac)-NH_2 and GLP-1(7–37)Lys(PEGCys)-NH_2 conjugates was appreciated. In this regard, an evident increase in gold retention for GLP-1(7–37)Lys(PEGCys)-NH_2 conjugate to AuNPs (0.016% when gold concentrations about 200 μg/mL were tested) was observed (Table SI-5).

Interestingly, in this model, AuNPs conjugated to GLP-1(7–37)Lys(Cys)-NH_2 did not improve penetration when cells were incubated for 4 h (Table SI-5). This result suggests that the incorporation of a PEG sequence as spacer is important for improving cell penetration/biocompatibility of functionalized AuNPs. In fact, some authors have reported that the incorporation of PEG chains conjugated to the surface of AuNPs attached with pharmacologically active molecules facilitate the gastrointestinal absorption of AuNPs. The absorption would be influenced by the PEG and type of ligand used to functionalized AuNPs, with low molecular weight derivatives (∼400 g/mol) giving the best permeability results [36,37].

On the other hand, several authors have reported that AuNP absorption depends largely on the size, surface charge and coating material [38,39]. In the present study, we have shown that the interaction between the coating material and the gold surface also significantly affects the behaviour of particles under physiological conditions, since weak interactions between ligands and AuNPs, as occurred in the conjugate to GLP-1(7–37)Lys(Ac)-NH_2, leads to an easier ligand exchange when AuNPs are exposed to an environment rich in proteins, such as that of the *mucus* layer of the epithelium. The presence of weak interactions between the ligand and the surface of the particles would explain why AuNPs conjugated to GLP-1(7–37)Lys(Ac)-NH_2 were mostly outside the cells compared to PEG-thiolated conjugate (Figs. SI-17 to SI-19).

In parallel to the permeability study, we performed some tests to evaluate the potential toxicity of the conjugates on the cell monolayer. These results showed that the conjugates at an AuNP concentration of 10 and 20 nM did not affect the integrity of tight junctions (Fig. SI-20) and did not have negative effects on the metabolic activity (viability) of intestinal epithelial cells after 2 and 4 h of exposure (Fig. 5).

3.7. *Hypoglycemic activity* in vivo

As previously shown, all three GLP-1 analogues had similar *in vitro* insulinotropic activity; however, as revealed by the permeability assays, not all the conjugates were able to penetrate Caco-2 cells in the same way. This finding indicates that some of them would not be good candidates to cross biological barriers and therefore neither would they be suitable potential delivery systems. Therefore, to study *in vivo* hypoglycemic activity, we selected the conjugate of GLP-1(7–37)Lys(PegCys)-NH_2 to AuNPs, since it penetrated a higher proportion of Caco-2 cells than the others (see permeability assay section) and also showed good physical-chemical stability as this peptide was more efficient at coating the AuNP surface (see IR analysis and estimation of the number of peptide molecules per AuNP section).

As can be seen in Fig. 6A, glycemia values reached a maximum at 30 min and returned to normality after 2 h. At this

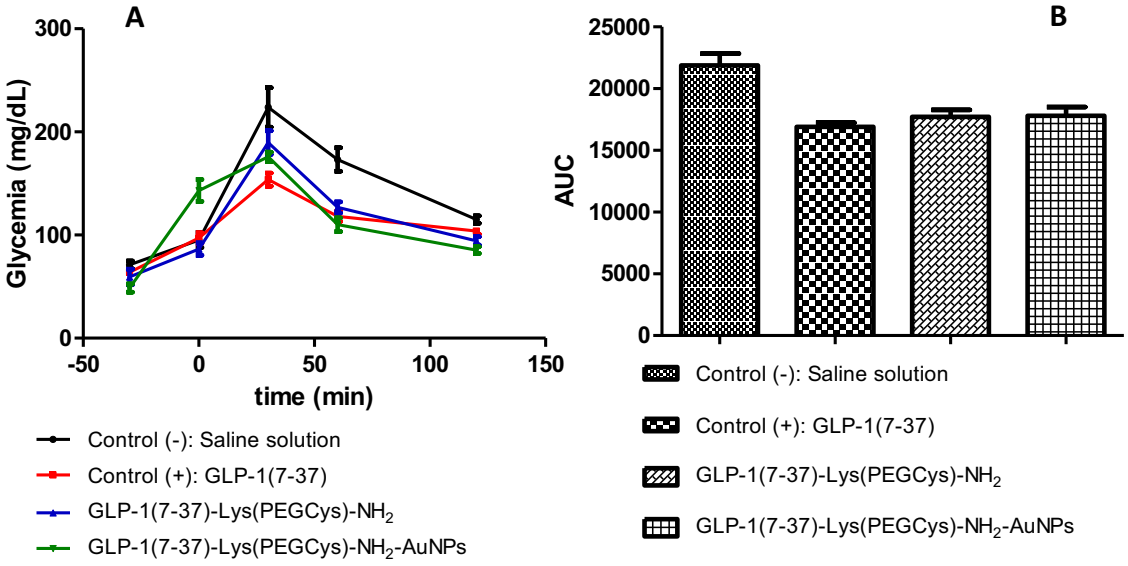

Fig. 6. (A) Glucose profiles obtained after oral administration of 2 g/kg glucose. Rats were pre-treated with: saline solution, GLP-1(7–37), GLP-1(7–37)-Lys(PEGCys)-NH_2, and GLP-1(7–37)-Lys(PEGCys)-NH_2 conjugated to AuNP. Results are expressed as mean ± SEM, n = 5. (B) AUC of the glycemic profiles obtained after oral administration of 2 g/kg glucose. Results are expressed as mean ± SEM, n = 5 ($p < 0.05$).

time, the glucose levels were: 104 ± 7 mg/mL for native GLP-1, 94 ± 9 mg/mL for the analogue GLP-1(7–37)Lys(PEGCys)-NH_2, 85 ± 7 mg/mL for conjugated AuNPs and 115 ± 8 mg/mL for the control. These values demonstrate that GLP-1(7–37)Lys(PEGCys)-NH_2 peptide conjugated to AuNPs is able to achieve a significantly greater decrease in blood glucose than the native GLP-1 (mean difference = 18.40; q = 5.270). This decrease was not observed after free GLP-1(7–37)Lys(PEGCys)-NH_2 administration. Indeed native GLP-1 and its analogue did not show statistical differences regarding blood glucose levels 2 h after intraperitoneal administration (mean difference = 9.40; q = 2.692). In addition, the analysis of the areas under the curve (AUC) revealed that there were no statistical differences among the three compounds tested, with hypoglycemic efficacy being 18.7 ± 6.7%, 22.1 ± 8.3% and 27.6 ± 6.3% for the GLP-1 analogue, endogenous incretin and the conjugate to AuNPs, respectively (Fig. 6B). On the basis of these results, we can conclude that the conjugation of a PEG-thiolated GLP-1 analogue to AuNPs is a physiologically stable system that can maintain the insulinotropic activity of this incretin and achieve a greater reduction of glycemia after 2 h of administration than that reached with the free peptide.

4. Conclusions

We have demonstrated that incretin GLP-1 can be used as a base to construct a GLP-1-AuNP conjugate with promising properties to be used as drug. An optimal modification of the GLP-1 sequence involves elongation at the C-terminal by a residue of amidated Lys, bearing in its ε-amino group a mini PEG spacer and Cys, whose thiol group binds to the AuNP by chemisorption providing improved capping of the gold surface, along with high stability. The incorporation of PEG is beneficial for improving biocompatibility with biological barriers and increases the absorption efficient of this conjugate when non-invasive administration routes are used. This construct proved stable and non-toxic for epithelial and pancreatic cells. Furthermore, it reduced glycemia levels, showing hypoglycemic efficacy similar to that of GLP-1. On the basis of our findings, we conclude that conjugation to AuNPs may provide an effective delivery system for GLP-1 and potential analogues.

Acknowledgements

The authors thank Dr. Fernanda Schaufler from the University of Chile for her assistance in evaluating the hypoglycemic effect in vivo, Dr. Fernando Ezquer from the University of Desarrollo for help evaluating the activity of the GLP-1 analogues, and Dr. Fanny Guzman for her assistance with the circular dichroism experiments. This study was supported by CONICYT ATD-24110090 (Chile) and AECID A1/035396/11 (Spain). Magdalena Pérez-Ortiz and Claudio Zapata-Urzúa are grateful to CONICYT for PhD fellowships and to the Vicerectory of Academic Issues (University of Chile) for the research stay fellowships. Marcelo J. Kogan is grateful to Fondap 15130011.

Appendix A. Supplementary data

Supplementary data associated with this article can be found, in the online version, at http://dx.doi.org/10.1016/j.colsurfb.2017.06.015.

References

[1] C. Orskov, L. Rabenhoj, A. Wettergren, H. Kofod, J.J. Holst, Tissue and plasma concentrations of amidated and glycine-extended glucagon-like peptide I in humans, Diabetes 43 (1994) 535–539, http://dx.doi.org/10.2337/diab.43.4.535.
[2] L.L. Baggio, D.J. Drucker, Biology of incretins: GLP-1 and GIP, Gastroenterology 132 (2007) 2131–2157, http://dx.doi.org/10.1053/j.gastro.2007.03.054.
[3] V. Gupta, Glucagon-like peptide-1 analogues: an overview, Indian J. Endocr. Metab. 17 (2013) 413–421, http://dx.doi.org/10.4103/2230-8210.111625.
[4] A. Peters, Incretin-based therapies review of current clinical trial data, Am. J. Me. 123 (2010) S28–S37, http://dx.doi.org/10.1016/j.amjmed.2009.12.007.
[5] A. Muheem, F. Shakeel, M.A. Jahangir, M. Anwar, N. Mallick, G.K. Jain, M.H. Warsi, F.J. Ahmad, A review on the strategies for oral delivery of proteins and peptides and their clinical perspectives, Saudi Pharm. J. 24 (2016) 413–428, http://dx.doi.org/10.1016/j.jsps.2014.06.004.
[6] B.J. Aungst, Absorption enhancers: applications and advances, AAPS J. 14 (2012) 11–18, http://dx.doi.org/10.1208/s12248-011-9307-4.
[7] L.R. Brown, Commercial challenges of protein drug delivery, Expert Opin. Drug Deliv. 2 (2005) 29–42, http://dx.doi.org/10.1517/17425247.2.1.29.
[8] P. Martins, D. Rosa, A.R. Fernandes, P.V. Baptista, Nanoparticle drug delivery systems: recent patents and applications in nanomedicine, Recent Patents Nanomed. 3 (2013) 1–14, http://dx.doi.org/10.2174/1877912304666140304000133.

[9] E.E. Connor, J. Mwamuka, A. Gole, C.J. Murphy, M.D. Wyatt, Gold nanoparticles are taken up by human cells but do not cause acute cytotoxicity, Small 1 (2005) 325–327, http://dx.doi.org/10.1002/smll.200400093.
[10] C.L. Villiers, H. Freitas, R. Couderc, M.B. Villiers, P.N. Marche, Analysis of the toxicity of gold nanoparticles on the immune system: effect on dendritic cell functions, J. Nanopart. Res. 12 (2009) 55–60, http://dx.doi.org/10.1007/s11051-009-9692-0.
[11] Y. Qu, X. Lu, Aqueous synthesis of gold nanoparticles and their cytotoxicity in human dermal fibroblast −fetal, Biomed. Mater. 4 (2009) 025007–025012, http://dx.doi.org/10.1088/1748-6041/4/2/025007.
[12] M.A. Dobrovolskaia, A.K. Patri, J.W. Zheng, J.D. Clogston, N. Ayub, P. Aggarwal, B.W. Neun, J.B. Hall, S.E. McNeil, Interaction of colloidal gold nanoparticles with human blood: effects on particle size and analysis of plasma protein binding profiles, Nanomedicine 5 (2009) 106–117, http://dx.doi.org/10.1016/j.nano.2008.08.001.
[13] P. Ghosh, G. Han, M. De, C.K. Kim, V.M. Rotello, Gold nanoparticles in delivery applications, Adv. Drug Deliv. Rev. 60 (2008) 1307–1315, http://dx.doi.org/10.1016/j.addr.2008.03.016.
[14] H. Gu, P.L. Ho, E. Tong, L. Wang, B. Xu, Presenting vancomycin on nanoparticles to enhance antimicrobial activities, Nano Lett. 3 (2003) 1261–1263, http://dx.doi.org/10.1021/nl034396z.
[15] B. Saha, J. Bhattacharya, A. Mukherjee, A. Ghosh, Ch.R. Santra, A.K. Dasgupta, P. Karmakar, In vitro structural and functional evaluation of Au nanoparticles conjugated antibiotics, Nanoscale Res. Lett. 2 (2007) 614–622, http://dx.doi.org/10.1007/s11671-007-9104-2.
[16] Y.H. Chen, C.Y. Tsai, P.Y. Huang, Chang, P.C. Cheng, C.H. Chou, D.H. Chen, C.R. Wang, A.L. Shiau, C.L. Wu, Methotrexate conjugated to Au nanoparticles inhibits tumor growth in a syngeneic lung tumor model, Mol, Pharm. 4 (2007) 713–722, http://dx.doi.org/10.1021/mp060132k.
[17] Y. Cheng, A.C. Samia, J.D. Meyers, I. Panagopoulos, B. Fei, C. Burda, Highly efficient drug delivery with gold nanoparticle vectors for in vivo photodynamic therapy of cancer, J. Am. Chem. Soc. 130 (2008) 10643–10647, http://dx.doi.org/10.1021/ja801631c.
[18] L. Hosta, M. Pla-Roca, J. Arbiol, C. López-Iglesias, J. Samitier, L.J. Cruz, M.J. Kogan, F. Albericio, Conjugation of kahalalide F with gold nanoparticles to enhance in vitro antitumoral activity, Bioconjugate Chem. 20 (2009) 138–146, http://dx.doi.org/10.1021/bc800362j.
[19] H.M. Joshi, D.R. Bhumkar, K. Joshi, V. Pokharkar, M. Sastry, Gold nanoparticles as carriers for efficient transmucosal insulin delivery, Langmuir 22 (2006) 300–305, http://dx.doi.org/10.1021/la051982u.
[20] D.R. Bhumkar, H.M. Joshi, M. Sastry, V.B. Pokharkar, Chitosan reduced gold nanoparticles as novel carriers for transmucosal delivery of insulin, Pharm. Res. 24 (2007) 1415–1427, http://dx.doi.org/10.1007/s11095-007-9257-9.
[21] S. Jain, D.G. Hirst, J.M. O'Sullivan, Gold nanoparticles as novel agents for cancer therapy, Br. J. Radiol. 85 (2012) 101–113, http://dx.doi.org/10.1259/bjr/59448833.
[22] I. Olmedo, E. Araya, F. Sanz, E. Medina, J. Arbiol, P. Toledo, A. Alvarez-Lueje, E. Giralt, M.J. Kogan, How changes in the sequence of the peptide CLPFFD-NH2 can modify the conjugation and stability of gold nanoparticles and their affinity for β-amyloid fibrils, Bioconjugate Chem. 19 (2008) 1154–1163, http://dx.doi.org/10.1021/bc800016y.
[23] International Standard ISO 22412:2008. Particle Size Analysis—Dynamic Light Scattering (DLS); Updates and extends ISO 13321:1996. Particle Size Analysis-Photon Correlation Spectroscopy.
[24] M. Smoluchowski, Handbuch der Electrizität und des Magnetismus (Graetz) vol. II. Leipzig, Germany: Barth; 1921. p. 366.
[25] X. Liu, M. Atwater, J. Wang, Q. Huo, Extinction coefficient of gold nanoparticles with different sizes and different capping ligands, Colloids Surf. B Biointerfaces 58 (2007) 3–7, http://dx.doi.org/10.1016/j.colsurfb.2006.08.005.
[26] Test Solutions, United States Pharmacopeia 35, NF 30, 2012.
[27] R. López de Maturana, D. Donnelly, The glucagon-like peptide-1 receptor binding site for the N-terminus of GLP-1 requires polarity at Asp198 rather than negative charge, FEBS Lett. 530 (2002) 244–248, http://dx.doi.org/10.1016/S0014-5793(02)03492-0.
[28] D. Donnelly, The structure and function of the glucagon-like peptide-1 receptor and its ligands, Br. J. Pharmacol. 166 (2012) 27–41, http://dx.doi.org/10.1111/j. 1476-5381.2011.01687.x.
[29] A. Wettergren, L. Pridal, M. Wojdemann, J.J. Holst, Amidated and non-amidated glucagon-like peptide-1 (GLP-1): non-pancreatic effects (cephalic phase acid secretion) and stability in plasma in humans, Regul. Pept. 77 (1998) 83–87, http://dx.doi.org/10.1016/S0167-0115(98)00044-5.
[30] K. Thornton, D.G. Gorenstein, Structure of glucagon-like peptide (7–36) amide in a dodecylphosphocholine micelle as determined by 2D NMR, Biochemistry 33 (1994) 3532–3539, http://dx.doi.org/10.1021/bi00178a009.
[31] N.H. Andersen, Y. Brodsky, J.W. Neidigh, K.S. Prickett, Medium-dependence of the secondary structure of exendin-4 and glucagon-like-peptide-1, Bioorgan. Med. Chem. 10 (2002) 79–85, http://dx.doi.org/10.1016/S0968-0896(01)00263-2.
[32] E. Sebokova, A.D. Christ, H. Wang, S. Sewing, J.Z. Dong, J. Taylor, M.A. Cawthorne, M.D. Culler, Taspoglutide, an analog of human glucagon-like peptide-1 with enhanced stability and in vivo potency, Endocrinology 151 (2010) 2474–2482, http://dx.doi.org/10.1210/en.2009-1459.
[33] A. Majzik, L. Fülöp, E. Csapó, F. Bogár, T. Martinek, B. Penke, G. Bíró, I. Dékány, Functionalization of gold nanoparticles with amino acid, beta-amyloid peptides and fragment, Colloids Surf. B Biointerfaces 81 (2010) 235–241, http://dx.doi.org/10.1016/j.colsurfb.2010.07.011.
[34] L. Vigderman, E.R. Zubarev, Therapeutic platforms based on gold nanoparticles and their covalent conjugates with drug molecules, Adv. Drug Deliv. Rev. 65 (2013) 663–676, http://dx.doi.org/10.1016/j.addr.2012.05.004.
[35] T.F. Tadros, Colloid Stability The Role of Surface Forces—Part I, Volume 1. 2006. ISBN: 978-3-527-31462-1.
[36] M.D. Donovan, G.L. Flynn, G.L. Amidon, Absorption of polyethylene glycols 600 through 2000: the molecular weight dependence of gastrointestinal and nasal absorption, Pharm. Res. 7 (1990) 863–868, http://dx.doi.org/10.1023/A:1015921101465.
[37] C.A. Smith, C.A. Simpson, G. Kim, C.J. Carter, D.L. Feldheim, Gastrointestinal bioavailability of 2. 0 nm diameter gold nanoparticles, ACS Nano 7 (2013) 3991–3996, http://dx.doi.org/10.1021/nn305930e.
[38] M. Liang, I.C. Lin, M.R. Whittaker, R.F. Minchin, M.J. Monteiro, I. Toth, Cellular uptake of densely packed polymer coatings on gold nanoparticles, ACS Nano 4 (2010) 403–413, http://dx.doi.org/10.1021/nn9011237.
[39] C. Schleh, M. Semmler-Behnke, J. Lipka, A. Wenk, S. Hirn, M. Schäffler, G. Schmid, U. Simon, W.G. Kreyling, Size and surface charge of gold nanoparticles determine absorption across intestinal barriers and accumulation in secondary target organs after oral administration, Nanotoxicology 6 (2012) 36–46, http://dx.doi.org/10.3109/17435390.2011.552811.